Undergraduate Journal of Experimental Microbiology and Immunology (UJEMI) Vol. 27:1-13

Towards optimizing ATP-induced activation of the NLRP3 inflammasome in glycolysis-inhibited J774A.1 murine macrophages

Helia Mansouri Dana, Ariel Rosen and Parsa Tabassi

Department of Microbiology and Immunology, University of British Columbia, Vancouver, British Columbia, Canada

SUMMARY Persistent inflammatory reactions underlie many of the physiological changes observed during aging. During the aging process, levels of self-antigens such as extracellular ATP increase and induce homeostatic changes as well as the activation of the NLRP3 inflammasome, a multi-protein complex containing the NLRP3 sensor protein which becomes activated in response to foreign pathogens and tissue damage. Aberrant inflammasome activation contributes to the aging process and has been linked to metabolic disturbances, though the exact mechanism for this remains unclear. An exploration of the link between cellular metabolic changes and inflammatory responses to age-associated molecules would provide further insight into the interplay between chronic inflammation and aging. In this study, we attempted to describe this interaction by inhibiting glycolysis in J774A.1 murine macrophages with 2-deoxyglucose (2-DG) and glucose 6-phosphate (G6P), and quantifying NLRP3 inflammasome activation using the production of cleaved IL-1β. Through Western blot, ELISA, and cell morphology analysis, we observed pro-IL-1β upregulation following LPS priming of J774A.1 cells, but were unable to detect cleaved IL-1β and observe distinctive cell morphology changes following ATP treatment. Glycolysis inhibition using 2-DG and G6P was also unsuccessful, as confirmed via a glycolysis assay.

INTRODUCTION

Cells of the innate immune system contain many response cascades and signaling pathways which dictate their responses to foreign and intrinsic stimuli. Both pathogen-associated molecular patterns (PAMPs) and damage-associated molecular patterns (DAMPs) have been shown to stimulate leukocytes and induce a variety of inflammatory responses, with one emergent component of this response being the formation of inflammasomes (1, 2). Inflammasomes are multi-protein complexes that generate an inflammatory response through the activation of caspase proteins, with the specific caspase protein activated dictating the resulting response pathway (1). Activation of caspase 1 constitutes the canonical pathway, while activation of caspase 11 leads to the non-canonical pathway (1). Following inflammasome activation through either the canonical or non-canonical pathway, leukocytes undergo a distinct response characterized by the secretion of pro-inflammatory cytokines such as IL-1β and IL-18, and pyroptosis, a form of lytic cell death (3). IL-1β and IL-18 are potent inflammatory cytokines secreted during various critical host responses to infection, with IL-1β being particularly important due to its general regulation of inflammation (2). IL-1β is secreted in its cleaved, mature form from its predecessor pro-IL-1β and can be identified via protein detection methods such as enzyme-linked immunosorbent assays (ELISA) or Western blots, while pyroptosis can be visually confirmed by the presence of bubble-like bodies in the plasma membranes of cells which result in a distinctive ballooned morphology (4). To further understand inflammasome-mediated responses and their involvement in overall inflammatory responses, an analysis of the inflammasome's key components is necessary.

A critical component of the inflammasome is NOD-, LRR- and pyrin domain-containing protein 3 (NLRP3), a cytosolic innate immune sensor which oligomerizes upon activation to form the inflammasome and takes part in both the canonical and non-canonical pathways (1). In macrophages, NLRP3 activators alone are not sufficient to induce inflammasome activation, and a priming signal (signal 1) is required (2, 5). Priming stimuli can be ligands

Published Online: September 2022

Citation: Mansouri Dana, Rosen, and Tabassi. 2022. Towards optimizing ATP-induced activation of the NLRP3 inflammasome in glycolysis-inhibited J774A.1 murine macrophages. UJEMI 27:1-13

Editors: Andy An and Gara Dexter, University of British Columbia

Address correspondence to: https://jemi.microbiology.ubc.ca/

for toll-like receptors, NLRs, or cytokine receptors, which activate the transcription factor NF-kB (2, 5). In turn, NF-kB upregulates NLRP3 and pro-IL-1β, which are not constitutively expressed in resting macrophages (2, 5). Following this priming step, the NLRP3 can be activated by a wide range of stimuli, including host- pathogen-, and environment-derived molecules (2). NLRP3 activation results in the proteolytic activation of caspase-1 (downstream of the canonical pathway) which in turn cleaves pro-IL-1β into its mature form IL-1β (1, 5, 6). Thus, upregulation of NLRP3, cleaved caspase-1, and cleaved IL-1β serve as helpful readouts for inflammasome activation (1). Although NLRP3 is activated by this array of stimuli, the formation of the NLRP3 inflammasome does not seem critical for many host defense mechanisms *in vivo*, likely due to redundancy with other inflammasomes (7–9). However, NLRP3 plays a non-redundant pathological role in several inflammatory diseases such as type 2 diabetes and multiple sclerosis (10). Thus, if NLRP3 is not essential to host defense mechanisms, this raises the question of what other physiological functions NLRP3 plays in healthy individuals. Recognizing the other physiological functions of NLRP3 may elucidate the role of NLRP3 in inflammatory disease.

NLRP3 has been shown to play a physiological role as a sensor of altered cellular homeostasis in response to cellular stress (11). One stressor that can lead to homeostatic disturbances is the process of aging. Aging is characterized by cell senescence, during which the cell cycle is arrested and the levels of many age-associated DAMPs are elevated (12, 13). One key age-related DAMP which has been shown to activate NLRP3 is extracellular ATP (12). The presence and recognition of extracellular ATP by immune cells results in low-grade chronic inflammation which may instigate age-related functional decline and may be at the forefront of the relationship between aging and the development of chronic diseases such as diabetes, atherosclerosis and arthritis (10). Thus, an exploration of the role of the NLRP3 inflammasome in the context of aging could prove to be invaluable.

Aside from low-grade inflammation, another key feature associated with altered homeostasis during aging is metabolic disturbance (11). For example, disrupted cellular homeostasis as a result of aging may lead to modifications in the cell such as a shift in cellular metabolism from oxidative phosphorylation to glycolysis (14, 15). The switch to glycolysis due to cell stress has been linked to NLRP3 inflammasome function, though the exact mechanism underlying this relationship remains unclear (1, 16, 17). Inhibition of the glycolytic enzyme hexokinase using 2-DG was shown to inhibit transcription of IL-1β in LPS-stimulated macrophages (18). Acting as a D-glucose mimic, 2-DG inhibits glycolysis by causing accumulation of 2-deoxy-d-glucose-6-phosphate (2-DG6P), which inhibits the function of hexokinase and glucose-6-phosphate isomerase, ultimately inhibiting glycolysis (19). Another study, however, found that hexokinase inhibition by G6P led to increased NLRP3 activation and increased expression of IL-1β in peptidoglycan (PG)-stimulated macrophages (20). G6P is the enzymatic product of hexokinase and the addition of G6P leads to feedback inhibition of hexokinase and thus prevents glycolysis (20). As such, we hypothesized that 2-DG and G6P treatment of LPS-primed, ATP-stimulated J774A.1 macrophages facilitates direct analysis of the effects of glycolysis inhibition in activating the NLRP3 inflammasome, detected through cleaved IL-1β production.

In this study, we explored the mechanisms by which the age-associated DAMP ATP contributes to the metabolic switch to glycolysis during cellular homeostatic disturbances related to aging. Specifically, we directly compared NLRP3 inflammasome activation following glycolysis inhibition using 2-DG and G6P using cleaved IL-1β production in LPS-primed, ATP-activated J774A.1 cells, in an attempt to reveal the mechanistic pathways linking DAMPs, glycolysis, and NLRP3 inflammasome activation. Our results showed pro-IL-1β production following LPS priming of J774A.1 cells, but we were unsuccessful in building upon these findings as we did not observe cleaved IL-1β production or the characteristic ‘bubbling’ morphology described during NLRP3 inflammasome activation and pyroptosis. Despite the inconclusiveness of our findings, this study provides valuable insight into the use of the J774A.1 murine macrophage model for analyzing NLRP3 inflammasome activation in glycolysis inhibited conditions, and can be built upon in future studies to obtain more conclusive results.

METHODS AND MATERIALS

Reagent Preparation. LPS (*Escherichia coli*) (Sigma-Aldrich, Cat no. L4391) available in stocks of 1mg/µl was used for cell stimulation and initial priming. For the second signal of NLRP3 inflammasome activation, ATP (Sigma-Aldrich, Cat no. A2383-1G) and nigericin (Millipore Sigma, Cat no. N7143-5MG) were used and solutions were prepared in PBS for a concentration of 5mM and 10µM, respectively. ATP solution was adjusted to pH 7 using 1N NaOH. Glycolysis inhibitors G6P (Sigma-Aldrich, Cat no. 10127647001) and 2-DG (Sigma-Aldrich, Cat no. D3875-1g) were dissolved in PBS pH 7.2 for final stock concentrations of 2M and filter sterilized. All powders were added according to solute solubility in PBS (G6P=10mg/ml; 2-DG=10mg/ml; ATP=50mg/ml; nigericin=0.15mg/ml - recommended in 1:5 ethanol to PBS solution but was dissolved in PBS in this experiment). Triton X-100 lysis buffer was prepared using 20mM Tris (pH 8.8), 127mM NaCl, 10% glycerol, 1% Triton X-100, 2mM EDTA, and distilled H_2O. ELISA wash buffer was prepared using 1X PBS and 0.05% Tween-20, and 1M H_3PO_4 was used as stop buffer (Thermo Fisher, Cat no. SS04). Sample loading buffer (4X) was pre-made using 0.25 M Tris-HCl pH 6.8, 8% SDS, 30% Glycerol, and 0.02% Bromophenol Blue containing 0.3M DTT.

J774A.1 Cell Culture. Mouse J774A.1 macrophages (Kronstad Lab, Michael Smith Laboratories, UBC) were cultured in Dulbecco's Modified Eagle Medium (DMEM) containing 10% (v/v) fetal bovine serum (FBS) (Thermo Fisher GibCo™, Cat no. 10438026) and 2mM GlutaMAX™ L-glutamine (Thermo Fisher, Cat no. 35050061). For initial passages, cells were split every 48 hours into T25 flasks at a ratio of 1:3 in DMEMc. Cells from passages 3 to 6 were frozen in 5% DMSO, diluted in complete media. Stimulations for each round of experimentation were done using cells from the same passages (Round 1: passage 3; Rounds 2 & 3: passage 4) to ensure consistency. J774A.1 cells were cultured in T75 flasks at 1:3 ratio of cell suspension to DMEMc and grown for 72-96 hours in 37°C (5% CO_2) incubator to reach desired confluency for cell seeding; cell media were changed as needed. Cells were seeded in 6-well plates ($3.0x10^5$ cells per well) for Western Blot analysis, 24-well plates for ELISA ($5.0x10^4$ cells per well), and 96-well plates for glycolysis assay ($1.0x10^4$ cells per well), at 1:3 cell suspension to DMEMc ratio (https://www.thermofisher.com/ca/en/home/references/gibco-cell-culture-basics/cell-culture-protocols/cell-culture-useful-numbers.html). Seeded cells were grown for 48-72 hours in a 37°C (5% CO_2) incubator. To ensure cell health, cells were observed using a phase-contrast microscope.

Cell Stimulation. All stimulations were done in a 37°C (5% CO_2) incubator. Seeded J774A.1 macrophages were treated with 5000ng/ml LPS or an equivalent volume of 1X PBS (negative control) in DMEMc for 4 hours (Figure 1). J774A.1 macrophages (6-well and 24-well plates) were pre-treated with 0.5mM 2-DG, 0.5mM G6P, or 1X PBS (negative control for glycolysis inhibition) in DMEMc for 2 hours (Figures 2 & 3). Following glycolysis inhibition, cells were treated with 500ng/ml LPS or an equivalent volume 1X PBS (negative control) in DMEMc for 4 hours. For the second activation signal of NLRP3 inflammasome, macrophages were treated with ATP (5mM), nigericin (10µM), and 1X PBS (negative control) in DMEMc for 30 minutes. For the glycolysis assay (Figure 2C), cells were treated with 2-DG and G6P (serially diluted (½) concentrations from 0.5M to 0.125mM) and 1X PBS in serum-free DMEM for 2 hours, followed by LPS (500ng/ml) treatment for 4 hours in serum-free DMEM. ATP (5mM) and nigericin (10µM) were added in serum-free DMEM for a 30-minute incubation.

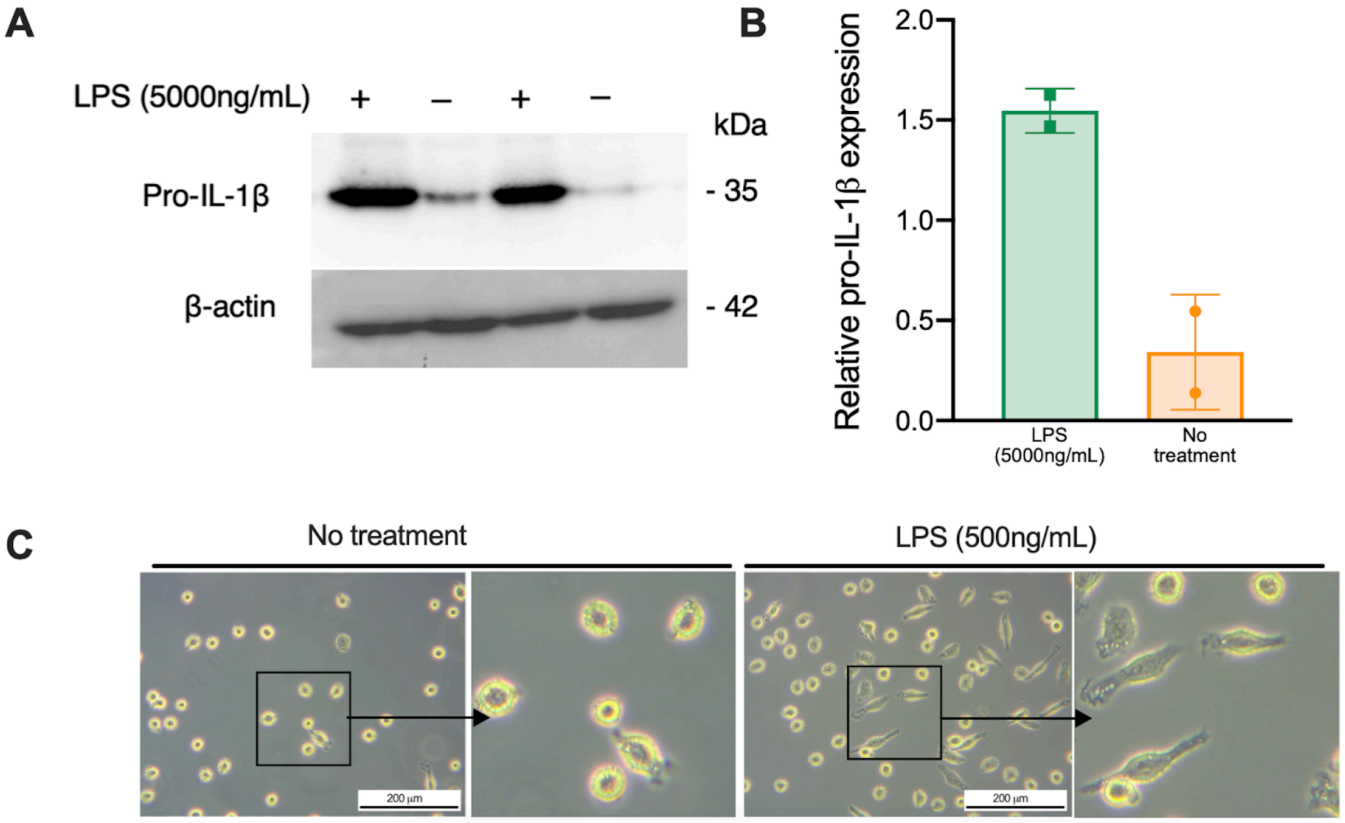

FIG. 1 Expression of pro-IL-1β increases with LPS stimulation in J774A.1 macrophages. (A) Western Blot analysis for pro-IL-1β of cell lysates from J774A.1 macrophages treated with LPS (5000ng/mL) for 4 hours or left untreated. β-actin served as the standard. (B) Densitometry analysis (n = 2) of pro-IL-1β expression relative to the β-actin standard for each of the conditions, performed in ImageJ. Data are shown as mean with SD. (C) Phase contrast images (scale bar = 200 µM) of untreated J774A.1 cells (left) and J774A.1 cells treated with 500ng/mL LPS for 4 hours, showing an elongated morphology (right). Insets created in Prism 9.0.2 (Materials and Methods, "Microscopy") and the box indicates the outline of the enlarged image.

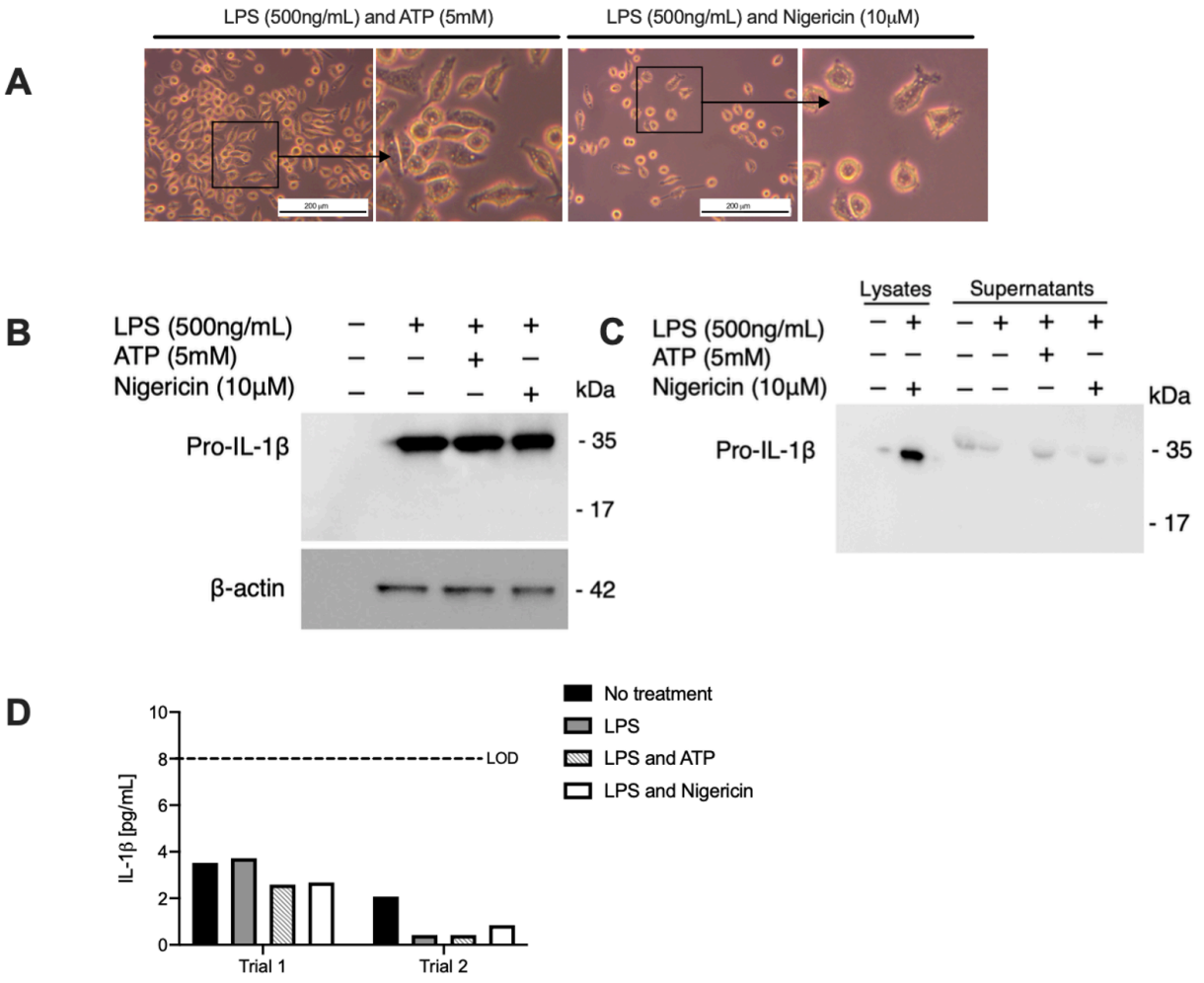

FIG. 2 Cleaved IL-1β is not detected under chosen experimental conditions via western blot or ELISA. (A) Phase contrast images (scale bar = 200 μM) of J774A.1 cells after LPS-stimulation (4 hours; 500ng/mL) followed by 30 minute 5mM ATP (left) or 10 μM nigericin (right) activation. Insets created in Prism 9.0.2 (Materials and Methods, "Microscopy") and the box indicates the outline of the enlarged image. (B) Western blot analysis for IL-1β in cell lysates of J774A.1 cells, treated as indicated. 12 μg of protein loaded for the complete negative condition, and 30 μg of protein loaded for all other conditions. β-actin served as the standard. (C) Western blot analysis for IL-1β from cell lysates and cell supernatants of J774A.1 cells treated as indicated. (D) Levels of IL-1β in cell supernatants of J774A.1 cells treated as indicated and analyzed via ELISA in two independent trials. Lower limit of detection (LOD) of the ELISA kit is indicated by a dashed line.

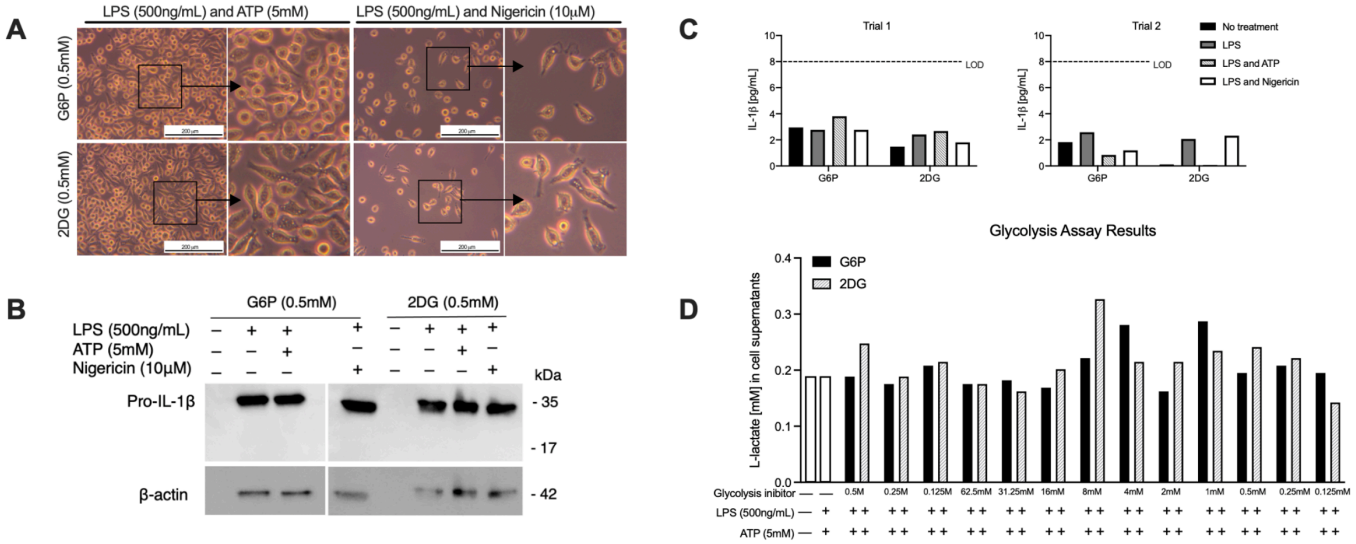

FIG. 3 -DG and G6P inhibition of glycolysis in LPS-stimulated, ATP- or nigericin-activated J774A.1 cells shows inconclusive results. (A) Phase contrast images (scale bar = 200 μM) of J774A.1 cells after 2-DG or G6P pre-treatment (2 hours), LPS-stimulation (4 hours), and ATP or nigericin activation (30 minutes), at the indicated concentrations. Insets created in Prism 9.0.2 (Materials and Methods, "Microscopy") and the box indicates the outline of the enlarged image. (B) Western blot analysis for IL-1β in cell lysates of J774A.1 cells, treated as indicated. 12 μg of protein loaded for the complete negative condition, and 30 μg of protein loaded for all other conditions. β-actin served as the standard. (C) Levels of IL-1β in cell supernatants of J774A.1 cells treated as indicated and analyzed via ELISA in two independent trials. Lower limit of detection (LOD) of the ELISA kit is indicated by a dashed line. (D) Glycolysis assay for the detection of L-lactate in J774A.1 supernatants treated as indicated. 1:2 dilutions of each glycolysis inhibitor were performed starting at 0.5M and ending at 0.125mM.

Microscopy. After pre-treatment and stimulation, images of J774A.1 cells were acquired using an inverted phase-contrast microscope (Zeiss Primovert) with the 40X objective fitted with an Axiocam ERc5s (Zeiss). Insets of images were created in Prism 9.0.2 by cropping a copy of each original image to the size indicated by the black box (identical box for each inset), then enlarging each cropped image to the same size.

Lysis Sample Preparation for Protein Analysis. J774A.1 cells were lysed using one cOmplete tablet (Sigma Aldrich, Cat no. 05892970001) dissolved in Triton X-100 Lysis Buffer. Pseudoreplicates (2 wells from the 6-well plate) were combined and collected in 100 μl lysis buffer to increase protein yield. Total protein was quantified using the Pierce™ BCA Protein Assay (Thermo Fisher, Cat no. 23225) according to the manufacturer's instructions. Pilot experiment: 20μg and 10μg of LPS-treated and PBS-treated cells were prepared for gel loading. Main experiment: maximal protein mass was prepared to load for each well, including 12.5μg of protein for negative control, PBS-treated samples and 30μg of protein for all other conditions. All samples were loaded with 1X Sodium-dodecyl Sulfate Polyacrylamide Gel Electrophoresis (SDS-PAGE) sample buffer.

Supernatant Sample Preparation for Protein Analysis. From stimulated J774A.1 cell cultures, cell supernatants were extracted and frozen at -20°C. Based on a protein concentration protocol from Chiu et al. (21), 300μl of cell supernatants were mixed with 300μl methanol and 125 μl chloroform at room temperature in a fume hood, and vortexed. 300μl distilled H_2O was added, and the mixture was incubated on ice for 10 minutes, centrifuged for 10 minutes at 13000 RPM at 4°C, and supernatants were discarded. An additional 500μl methanol was added to the pellet and mixed by vortexing. Centrifugation was repeated and supernatants were removed. Pellets were dried at 55°C and then dissolved in 20μl 1X SDS-PAGE Loading buffer. Samples were incubated at 95°C for 30 minutes,

followed by 1-2 minutes on ice. An additional 13µl of 1X loading buffer was then added, and samples were briefly spun down in preparation for gel electrophoresis.

SDS-PAGE. All samples were loaded onto a 12% (resolving) and 4% (stacking) polyacrylamide gel. For each gel run, the Precision Plus Protein Kaleidoscope ladder (Bio-Rad, Cat no. 161-0375) was loaded to determine protein band sizes. SDS-PAGE was conducted for band separation at 100V for 45 minutes (lysis samples) and 120V for 45 minutes (supernatant samples).

Western Blot Analysis. Protein transfer onto PVDF membranes was done overnight at 30V. Membranes were washed using TBS-T (Tris Buffer Saline with Tween 20), and incubated in Ponceau S Staining Solution for 5-10 minutes at room temperature for initial band visualization, using a platform shaker. Washing steps with TBS-T were repeated, and membranes were blocked using 5% milk. Incubation with monoclonal mouse anti-β-actin for mouse (A5316, Sigma Aldrich) diluted at 1:5000 1% milk-TBS-T solution followed for 90 minutes. Monoclonal rabbit anti-goat secondary antibody (Jackson ImmunoResearch, Cat. No AB_2339400) for β-actin was diluted at 1:10000 for incubation for 45 minutes. For detection of IL-1β, membranes were stripped, blocked with 5% milk, and incubated with polyclonal goat primary anti-IL-1β for mouse (R&D Systems, Cat no. AF-401-NA) diluted at 1:1000 in 1% milk-TBS-T solution for 90 minutes. Incubation with polyclonal goat anti-mouse IgG secondary antibody-HRP conjugate (Invitrogen, Cat no. 31430) was then done at a dilution of 1:15000 in 1% milk-TBS-T. Membranes were visualized using the Chemi-doc Imaging System (Bio-Rad). All incubations were done at room temperature.

ELISA. Supernatants from stimulated J774A.1 cells (stored at -20°C) were thawed. Supernatants were measured for mouse IL-1β using the IL-1β Mouse Uncoated ELISA Kit (Thermo Fisher, Cat no. 88-7013-86), according to the manufacturer's instructions. Absorbance values at 570nm were subtracted from those at 450nm to obtain the adjusted absorbance values used for analysis, as recommended by the manufacturer. Cytokine concentrations were quantified based on an 8-point standard curve generated in GraphPad Prism 9.0.2 using a 4 parameter algorithm.

Glycolysis Assay. Cell supernatants from J774A.1 cells cultured and stimulated in 96-well plates were analyzed for the presence of (L)-lactate using the Glycolysis Cell-Based Colourimetric Assay Kit (Cayman Chemicals, Cat no. 600450), based on the manufacturer's instructions. Lactate concentrations were quantified at 490nm using a microplate reader, and an 8-point standard curve was generated in GraphPad Prism 9.0.2.
Figures. All figures were created in GraphPad Prism 9.0.2.

RESULTS

Stimulation of J774A.1 macrophages with LPS leads to increased expression of pro-IL-1β compared to unstimulated cells. To determine how J774A.1 macrophages respond to the priming signal of the NLRP3 inflammasome canonical pathway, we analyzed the production of pro-IL-1β in LPS-stimulated J774A.1 cells via western blot. We found that LPS stimulation of J774A.1 macrophages increased pro-IL-1β production compared to unstimulated cells (Fig. 1A). Via densitometry analysis, we observed that normalized to the respective β-actin controls, LPS-stimulated cells had 4.5-fold higher expression of pro-IL-β compared to untreated cells (Fig. 1B). Further, compared to untreated cells, LPS-stimulated cells displayed an elongated morphology with pseudopodia formation, which are characteristic morphological traits of pro-inflammatory macrophages (22) (Fig. 1C). Thus, a 4 hour, 5000ng/mL LPS stimulation is capable of priming the NLRP3 inflammasome in J774A.1 cells.

Chosen experimental conditions are not sufficient to detect cleaved IL-1β in J774A.1 macrophage lysates or supernatants. To investigate how age-related DAMPs activate the second signal of the canonical NLRP3 inflammasome pathway, we treated LPS-stimulated J774A.1 macrophages with ATP and with nigericin as a positive control. We examined cell morphology for signs of pyroptosis and assessed production and release of cleaved IL-1β as

proxies for NLRP3 inflammasome activation. LPS and ATP or nigericin treated cells displayed an elongated morphology (Fig. 2A), similar to the morphology of the LPS-only treated cells discussed above. However, we did not identify any overt signs of pyroptosis in LPS-stimulated, ATP- or nigericin-activated cells (Fig. 2A), such as membrane bubbling (3), indicating that the complete activation of the NLRP3 inflammasome may not have occurred.

We next analyzed lysates and supernatants from LPS-stimulated, ATP- or nigericin-activated J774A.1 macrophages for the production and release of cleaved IL-β as a proxy for full activation of the inflammasome. Pro-IL-1β was detected in both the lystates (Fig. 2B) and supernatants (Fig. 2C) of LPS-stimulated, ATP- or nigericin-activated J774A.1 cells via western blot, indicating a successful priming step of the NLRP3 inflammasome. No conclusions can be drawn regarding an increased production of pro-IL-1β relative to unstimulated cells due to the lack of protein loaded in the stimulated conditions, as exhibited by the lack of β-actin. Further, cleaved IL-1β could not be detected in the cell lysates or the cell supernatants via western blot, indicating that our chosen stimulation conditions are not suitable to induce the second signal of the canonical NLRP3 inflammasome pathway, or that our western blot analysis was not sensitive enough to detect the low levels of cleaved IL-1β that may have been produced in and/or released by the stimulated cells.

To differentiate between a lack of cleaved IL-1β release or an inability to detect cleaved IL-1β via western blot, we investigated levels of IL-1β in the cell supernatants of LPS-primed, ATP- or nigericin-activated J774A.1 cells via ELISA, to achieve higher sensitivity in detection. However, in two independent trials, we did not detect IL-1β within the detection limits of the assay (Fig. 2D). Therefore, because we did not detect cleaved IL-1β in the lysates or supernatants of LPS-primed, ATP- or-nigericin activated J774A.1 cells via western blot or the more sensitive ELISA, a thirty minute 5mM ATP or 10 μM nigericin stimulation may not be sufficient to activate the second signal of the NLRP3 inflammasome in J774A.1 cells.

2-DG and G6P inhibition of glycolysis shows inconclusive results with respect to NLRP3 inflammasome activation. To directly compare the effects of two inhibitors of the glycolytic enzyme HK-1 on the canonical NLRP3 inflammasome activation, we pre-treated J774A.1 macrophages with either 2-DG or G6P prior to priming the cells with LPS and then activating them with ATP or nigericin. To assess NLRP3 inflammasome activation in 2-DG or G6P pre-treated macrophages, we examined the cells morphologically and probed for cleaved IL-β via western blot and ELISA. We found that 2-DG and G6P treated cells displayed an elongated cell morphology with pseudopodia formation (Fig. 3A) in both the ATP and nigericin activation conditions, however, we did not observe the characteristic membrane bubbling of pyroptosis. Further, via western blotting, we found that pro-, but not cleaved, IL-β was expressed in 2-DG or G6P pre-treated, LPS-primed and ATP- or nigericin-activated J774A.1 cells (Fig. 3B). In two independent ELISA trials, we did not detect IL-1β within the detection limits of the assay (Fig. 3C). Therefore, either our chosen conditions were not sufficient to fully activate the canonical NLRP3 inflammasome in J774A.1 cells, or the inhibition of glycolysis by either 2-DG or G6P suppress NLRP3 inflammasome activation.

To discern if our glycolysis inhibitors were functioning to inhibit the glycolytic enzyme HK-1 in a dose-dependent manner, we conducted a glycolysis assay to assess the levels of L-lactate, the end product of glycolysis, in the supernatants of LPS-primed and ATP-activated J774A.1 cells alone or pre-treated with varying concentrations of 2-DG or G6P. We found minimal levels of L-lactate in all conditions (Fig. 3D). Levels of L-lactate were marginal even in the uninhibited cells, with less than 0.2mM of L-lactate detected in the cell supernatants (Fig. 3D). As a result, it is unsurprising that we could not detect a difference in L-lactate levels between glycolysis of uninhibited and inhibited cells, as the low levels of L-lactate detected overall suggest an issue with the assay. Because we cannot say for certain that our 2-DG and G6P pre-treatments of J774A.1 cells functioned to inhibit glycolysis, no conclusions can be drawn regarding the relationship between glycolysis and NLRP3 inflammasome activation in response to ATP.

DISCUSSION

In the pursuit of uncovering the pathway linking glycolysis and NLRP3 inflammasome activation in response to DAMPs, we were unsuccessful in observing significant

inflammasome activation in J774A.1 macrophages in response to ATP treatment following 2-DG and G6P glycolysis inhibition. We were able to observe a significant upregulation of pro-IL-1β production following LPS treatment, indicating that our cell model was indeed responding to our primary stimulus. Following our secondary stimulation with ATP or nigericin as a positive control, we observed a similar upregulation in pro-IL-1β, however, our results showed no detectable cleaved IL-1β in either treatment condition. We were further unable to detect cleaved IL-1β, despite the presence of pro-IL-1β in our supernatant analyses. Our analysis of glycolysis inhibition revealed unsuccessful inhibition of glycolysis, however, since our controls show a lack of NLRP3 inflammasome activation, this may indicate a lack of metabolic switch to glycolysis in the first place. Thus, our findings prove inconclusive and indicate a need for further optimization in future attempts.

Stimulation Conditions: First signal of NLRP3 inflammasome activation. The activation of the NLRP3 inflammasome complex requires a two-signal activation process, where specific PAMPs, namely bacterial LPS, provide the first priming signal for the upregulation of canonical inflammatory components such as pro-IL-1β (1). As seen in our results, LPS stimulation at the chosen concentration (5000 ng/ml) and time (4 hours) significantly upregulated expression of pro-IL-1β in J774A.1 macrophages compared to the PBS-treated controls (Fig. 1A & 1B), indicating successful priming of the NLRP3 inflammasome (2, 16). In addition, morphological changes in macrophages are correlated with macrophage polarization towards pro- or anti-inflammatory phenotypes, where an expanded or "pancake-like" cell is associated with the pro-inflammatory M1 phenotype in response to LPS stimulation and inflammasome activity (22, 23). In alignment with these reports, we found PBS-treated cells to be more circular (Fig. 1C), indicating a lack of activation and polarization in J774A.1 cells. However, LPS-treated J774A.1 cells had an expanded morphology with pseudopodia formation (Fig. 2A), indicating an activated pro-inflammatory phenotype. As such, the chosen LPS conditions within this experiment are likely sufficient for priming the NLRP3 inflammasome in J774A.1 macrophages.

Stimulation Conditions: Second signal of NLRP3 activation. The second activation signal for the NLRP3 inflammasome requires PAMPs or DAMPs, such as ATP and nigericin, to induce the formation of the inflammasome complex and lead to cell pyroptosis, a form of cell death characterized by a bubbling morphology (3). As seen in Fig. 3A, LPS-primed and ATP- or nigericin-activated J774A.1 cells do not display a bubbling cell shape; compared to Fig. 2A, the cells have an elongated and expanded form, which corresponds to a proinflammatory state induced by LPS stimulation. These results indicate a lack of NLRP3 inflammasome activation using the selected treatment conditions, and warrant further optimization of ATP and nigericin conditions in future experiments.

In addition, activation of the NLRP3 inflammasome leads to the cleavage of pro-IL-1β into the p17 subunit, mediated by the active form of caspase-1 after inflammasome assembly (1, 10). Cleaved IL-1β is a proinflammatory cytokine which, upon secretion, induces leukocyte trafficking to the site of inflammation (24). By increasing endothelial cell permeability and expression of adhesion molecules, IL-1β allows neutrophils and macrophages to arrest at the target tissue for extravasation (24). Contrary to reports in the literature, a treatment of 5mM ATP or 10μm nigericin for 30 minutes in LPS-primed macrophages did not yield detectable levels of cleaved IL-1β in our Western blots (Fig. 2B) (16, 25). We hypothesize that this may be due to limitations in the sensitivity of our Western blot analyses of lysates in detecting cleaved IL-1β. Using J774A.1 cells, a group reported loading 50 μg of total protein in each well for detection of IL-1β p17 after NLRP3 inflammasome activation (26). In our experiments, we loaded a maximal protein amount of around 30 μg, which may have been too low for adequate detection of cleaved IL-1β.

Alongside limitations in Western blot methodology, other groups have mainly used primary bone marrow-derived macrophages (BMDMs) to investigate NLRP3 inflammasome activation, and as such, we speculate that the described conditions in these papers may not have been sufficient to cause NLRP3 inflammasome activation in J774A.1 cells. One group reports a difference in inflammatory response in J774A.1 cells compared to BMDMs, claiming that J774A.1 macrophages tend to have slower and weaker responses to infection with *Mycobacterium tuberculosis* (27). While this variability is not directly shown with

respect to NLRP3 inflammasome activation, this may warrant further investigation to determine optimal conditions of ATP or nigericin treatment in J774A.1 cells compared to other cell types. As a result, we recommend a time-course and concentration-gradient experiment to identify optimal ATP and nigericin treatment for NLRP3 inflammasome activation in future experiments using J774A.1 cells. Using pro-IL-1β and cleaved IL-1β as outputs, these experiments can infer the effectiveness of the second activation signal of the NLRP3 inflammasome.

Analysis of cell supernatants. To detect cleaved IL-1β in the supernatants of LPS-primed, ATP-or nigericin-activated macrophages, we analyzed cell supernatants via western blot and ELISA. Contrary to other studies (19), cleaved IL-1β was not detected by western blot analysis of the cell supernatants (Fig. 2C). Interestingly, the study from which we based our protocol for the detection of protein in cell supernatants (19) detected cleaved IL-1β in the supernatants of J774A.1 cells primed with LPS (4 hours; 1μg/mL) and activated with ATP (0.5 hours; 1μg/ml). With only one experimental trial, it is difficult to discern why we did not see similar results under such comparable experimental conditions.

Regardless, our protocol may require optimization with respect to other methods of chloroform and methanol protein precipitation. Our selected protocol uses a methanol to sample ratio of 1:1, while other groups have reported using a ratio of 4:1, which may reduce contamination of protein samples with non-polar components, such as lipids and nucleic acids (28). Furthermore, researchers have reported higher protein yield using TCA precipitation and acetone extraction compared to methods using chloroform and methanol (29–31). Using the chloroform/methanol protocol, the supernatants did not fully dissolve in 1X SDS loading buffer and formed a jelly-like substance, indicating the presence of contaminating material such as DNA and lipids, which hindered our ability to load the full amount of protein prepared during the precipitation process. As outlined previously, cleaved IL-1β is difficult to detect in smaller amounts of loaded protein (26), and therefore, a modification of this protocol or an exploration of other protein extraction methods can aid to decrease contamination and enhance protein loading for more conclusive results.

Many groups report using the IL-1β Mouse Uncoated ELISA Kit (Thermo Fisher; Materials and Methods) to detect cleaved IL-1β as a measure of inflammasome activation using other stimulators such as prion peptides and niclosamide (32, 33), as well as using a 30-minute ATP (5 mM) or nigericin (10 μmol or 20 nM) incubation after LPS priming (200 ng/μl or 300 ng/ul) (25, 34–36). As such, we recommend trouble-shooting steps aimed at improving NLRP3 inflammasome activation during cell culture. Though reported LPS, ATP and nigericin stimulations are aligned with what was conducted in this project, our experiments yielded IL-1β readings below the threshold of detection in all conditions, excluding the standards, pointing to insufficient NLRP3 inflammasome activation (Fig. 2D). It should be noted, once more, that in the described literature, NLRP3 inflammasome activation was explored in primary bone marrow derived macrophages (BMDMs) (25, 32, 35), microglia (33), or B cells (36), presenting a limitation to its application to J774A.1 cells and providing a need for the optimization of cell response.

Additional attempts at ELISA optimization may concern the standard curve (Fig. S1), which deviated from the provided theoretical curve by Thermo Fisher. Namely, the highest concentration of the standard curve (1000 pg/ml) had absorbance readings of 0.76 and 0.18 at 450nm in the first and second rounds of ELISA compared to the theoretical absorbance reading of above 1.0, at the same wavelength (https://www.thermofisher.com/elisa/product/IL-1-beta-Mouse-Uncoated-ELISA-Kit-with-Plates/88-7013-86). This discrepancy is reflected in all other standard points, and the large variation of kit performance indicates poor kit handling or experimental errors. As signals were weaker than expected, it is recommended that the number of washes is increased to 5 times per wash step. Additionally, the plate is also recommended to be incubated with capture antibody overnight at 4°C instead of a shorter incubation time of 1 hour at room temperature, to increase assay sensitivity in future experiments.

Troubleshooting the Glycolysis Assay. The Glycolysis Cell-Based Assay by Cayman Chemicals offers a colorimetric detection of (L)-lactate, however, its use has not been reported in research investigating the NLRP3 inflammasome, instead used to examine the role of glycolysis in cancer and Parkinson's Disease (37–39). In our experiments, stimulation

conditions may not have been optimal to activate the NLRP3 inflammasome, and further, differences in lactate production within our glycolysis assay could not be detected between glycolysis inhibited and uninhibited cells (Fig. 3D). As such, our results are inconclusive in determining the relationship between glycolysis inhibition and NLRP3 inflammasome activation in LPS-primed and ATP/nigericin-stimulated J774A.1 macrophages. Furthermore, due to our limitations in detecting NLRP3 inflammasome activation, the chosen L-lactate colorimetric assay cannot be reliably assessed as an effective measurement of lactate production. However, after optimizing stimulation conditions, using assays validated for NLRP3 inflammasome analysis may be beneficial for future experiments.

Among assays used to investigate the role of glycolysis in NLRP3 inflammasome activity, researchers commonly use the SeaHorse XF Stress Kit to determine the extracellular acidification rate (ECAR) as a measure of glycolytic flux (16, 40–42). Furthermore, 2-DG, an HK-1 inhibitor, is a commonly used glycolysis inhibitor within these experiments, and recommended treatment concentrations vary at 0.5 mM (16), 10 mM (41), 50 mM (42), and 500 mM (40), depending on incubation times. Papers using lower concentrations of 2-DG pre-treated macrophages for 2 hours prior to ECAR measurement (16, 41); conversely, those using higher inhibitor concentrations injected 2-DG into cell media after sequential additions of glucose and oligomycin, which are used to increase or to inhibit metabolic activity, respectively, at 7 minute intervals (40, 42). In some papers, lactate colorimetric assays are included as supporting data alongside ECAR readings, with the BioVision assay used most prevalently. Methods further vary in sample preparation for this assay, as cells have been homogenized in one paper (42), while cell supernatants appear to have been used in others (16, 41). Generally, literature using these methods reported a consistent and significant decrease of NLRP3 activation upon HK-1 inhibition by 2-DG, marking the highlighted kits as reliable measures of glycolysis inhibition for future experiments.

Conclusions Taken together, our findings show inconclusive results concerning the role of glycolysis, namely the glycolytic enzyme HK-1, in NLRP3 inflammasome activation using age-related DAMPs such as ATP, and thus cannot contribute decisive results in the ongoing debate regarding metabolism and NLRP3 inflammasome function. Moving forward, pilot experiments aimed at finding the most effective ATP or nigericin stimulation conditions in LPS-primed J774A.1 macrophages will be necessary in ensuring NLRP3 inflammasome activation. Subsequently, glycolysis inhibition by 2-DG or G6P can be investigated using a variety of kits, with a preference to those already applied to inflammasome research. Lastly, implementing the discussed troubleshooting strategies in repeated trials of supernatant analysis via western blot and ELISA, and using the optimal NLRP3 stimulation conditions, can help to establish a relationship between glycolysis inhibition and NLRP3 inflammasome activity.

ACKNOWLEDGEMENTS

Vials of J774A.1 cells were a kind gift from the Kronstad lab, and we thank the Kronstad team for providing information regarding J774A.1 cell culture and maintenance. We further express gratitude to Dr. Marcia Graves for her knowledge, supervision, and continuous support throughout our experiments, Ameena Hashimi for her valuable guidance and feedback, Ms. Jade Muileboom for her technical guidance, and our MICB 421 peers for their reassurance and support throughout our experiments. This project was funded by the UBC Department of Microbiology and Immunology.

CONTRIBUTIONS

All participants participated equally in the project and in writing the manuscript. All three members invested an average of 24 hours per week at the UBC Microbiology and Immunology Laboratories. In completing the manuscript, A.R created and analyzed the figures, and wrote the results section. H.M completed the discussion section, and further described the methods used to complete this project. All three members conducted background research, and P.T and A.R completed the Introduction section based on the team's research. Lastly, P.T completed the Abstract of the project, and the team chose an appropriate title for the manuscript.

REFERENCES

1. **Swanson KV, Deng M, Ting JP-Y**. 2019. The NLRP3 inflammasome: molecular activation and regulation to therapeutics. *Nat Rev Immunol* **19**:477–489.
2. **Kelley N, Jeltema D, Duan Y, He Y**. 2019. The NLRP3 Inflammasome: An Overview of Mechanisms of Activation and Regulation. *Int J Mol Sci* **20**:3328.
3. **Jorgensen I, Miao EA**. 2015. Pyroptotic cell death defends against intracellular pathogens. *Immunological Reviews* **265**:130–142.
4. **Kayagaki N, Kornfeld OS, Lee BL, Stowe IB, O'Rourke K, Li Q, Sandoval W, Yan D, Kang J, Xu M, Zhang J, Lee WP, McKenzie BS, Ulas G, Payandeh J, Roose-Girma M, Modrusan Z, Reja R, Sagolla M, Webster JD, Cho V, Andrews TD, Morris LX, Miosge LA, Goodnow CC, Bertram EM, Dixit VM**. 2021. NINJ1 mediates plasma membrane rupture during lytic cell death. 7848. *Nature* **591**:131–136.
5. *Bauernfeind FG, Horvath G, Stutz A, Alnemri ES, MacDonald K, Speert D, Fernandes-Alnemri T, Wu J, Monks BG, Fitzgerald KA, Hornung V, Latz E*. 2009. Cutting Edge: NF-κB Activating Pattern Recognition and Cytokine Receptors License NLRP3 Inflammasome Activation by Regulating NLRP3 Expression. *The Journal of Immunology* **183**:787–791.
6. **Thornberry NA, Bull HG, Calaycay JR, Chapman KT, Howard AD, Kostura MJ, Miller DK, Molineaux SM, Weidner JR, Aunins J, Elliston KO, Ayala JM, Casano FJ, Chin J, Ding GJ-F, Egger LA, Gaffney EP, Limjuco G, Palyha OC, Raju SM, Rolando AM, Salley JP, Yamin T-T, Lee TD, Shively JE, MacCross M, Mumford RA, Schmidt JA, Tocci MJ**. 1992. A novel heterodimeric cysteine protease is required for interleukin-1βprocessing in monocytes. 6372. *Nature* **356**:768–774.
7. **Coll RC, O'Neill L a. J, Schroder K.** 2016. Questions and controversies in innate immune research: what is the physiological role of NLRP3? 1. *Cell Death Discovery* **2**:1–5.
8. **Chen KW, Schroder K**. 2013. Antimicrobial functions of inflammasomes. *Curr Opin Microbiol* **16**:311–318.
9. **Clay GM, Sutterwala FS, Wilson ME**. 2014. NLR proteins and parasitic disease. *Immunol Res* **59**:142–152.
10. **Guo H, Callaway JB, Ting JP-Y**. 2015. Inflammasomes: Mechanism of Action, Role in Disease, and Therapeutics. *Nat Med* **21**:677–687.
11. **Haneklaus M, O'Neill LAJ**. 2015. NLRP3 at the interface of metabolism and inflammation. *Immunol Rev* **265**:53–62.
12. **Youm Y-H, Grant RW, McCabe LR, Albarado DC, Nguyen KY, Ravussin A, Pistell P, Newman S, Carter R, Laque A, Münzberg H, Rosen CJ, Ingram DK, Salbaum JM, Dixit VD.** 2013. Canonical Nlrp3 inflammasome links systemic low-grade inflammation to functional decline in aging. *Cell Metab* **18**:519–532.
13. **Sebastian-Valverde M, Pasinetti GM**. 2020. The NLRP3 Inflammasome as a Critical Actor in the Inflammaging Process. *Cells* **9**:1552.
14. **Ganapathy-Kanniappan S, Geschwind J-FH**. 2013. Tumor glycolysis as a target for cancer therapy: progress and prospects. *Molecular Cancer* **12**:152.
15. **Feng Z, Hanson RW, Berger NA, Trubitsyn A**. 2016. Reprogramming of energy metabolism as a driver of aging. *Oncotarget* **7**:15410–15420.
16. **Moon J-S, Hisata S, Park M-A, DeNicola GM, Ryter SW, Nakahira K, Choi AMK**. 2015. mTORC1-Induced HK1-Dependent Glycolysis Regulates NLRP3 Inflammasome Activation. *Cell Reports* **12**:102–115.
17. **Krawczyk CM, Holowka T, Sun J, Blagih J, Amiel E, DeBerardinis RJ, Cross JR, Jung E, Thompson CB, Jones RG, Pearce EJ**. 2010. Toll-like receptor–induced changes in glycolytic metabolism regulate dendritic cell activation. *Blood* **115**:4742–4749.
18. **Tannahill GM, Curtis AM, Adamik J, Palsson-McDermott EM, McGettrick AF, Goel G, Frezza C, Bernard NJ, Kelly B, Foley NH, Zheng L, Gardet A, Tong Z, Jany SS, Corr SC, Haneklaus M, Caffrey BE, Pierce K, Walmsley S, Beasley FC, Cummins E, Nizet V, Whyte M, Taylor CT, Lin H, Masters SL, Gottlieb E, Kelly VP, Clish C, Auron PE, Xavier RJ, O'Neill L a. J**. 2013. Succinate is an inflammatory signal that induces IL-1β through HIF-1α. *Nature* **496**:238–242.
19. **Pajak B, Siwiak E, Sołtyka M, Priebe A, Zieliński R, Fokt I, Ziemniak M, Jaśkiewicz A, Borowski R, Domoradzki T, Priebe W.** 2019. 2-Deoxy-d-Glucose and Its Analogs: From Diagnostic to Therapeutic Agents. *Int J Mol Sci* **21**:E234.
20. **Wolf AJ, Reyes CN, Liang W, Becker C, Shimada K, Wheeler ML, Cho HC, Popescu NI, Coggeshall KM, Arditi M, Underhill DM**. 2016. Hexokinase Is an Innate Immune Receptor for the Detection of Bacterial Peptidoglycan. *Cell* **166**:624–636.
21. **Chiu H-W, Li L-H, Hsieh C-Y, Rao YK, Chen F-H, Chen A, Ka S-M, Hua K-F.** 2019. Glucosamine inhibits IL-1β expression by preserving mitochondrial integrity and disrupting assembly of the NLRP3 inflammasome. *Sci Rep* **9**:5603.
22. **McWhorter FY, Wang T, Nguyen P, Chung T, Liu WF**. 2013. Modulation of macrophage phenotype by cell shape. *Proceedings of the National Academy of Sciences* **110**:17253–17258.
23. **Wisitpongpun P, Potup P, Usuwanthim K**. 2022. Oleamide-Mediated Polarization of M1 Macrophages and IL-1β Production by Regulating NLRP3-Inflammasome Activation in Primary Human Monocyte-Derived Macrophages. *Frontiers in Immunology* **13**.

24. **Ren K, Torres R**. 2009. Role of interleukin-1β during pain and inflammation. *Brain Res Rev* **60**:57–64.
25. **Zhang L, Liu Y, Wang B, Xu G, Yang Z, Tang M, Ma A, Jing T, Xu X, Zhang X, Liu Y**. 2018. POH1 deubiquitinates pro-interleukin-1β and restricts inflammasome activity. *Nat Commun* **9**:4225.
26. **Hsieh C-Y, Li L-H, Lam Y, Fang Z, Gan CH, Rao YK, Chiu H-W, Wong W-T, Ju T-C, Chen F-H, Chernikov OV, Liu M-L, Hsu C-H, Hua K-F**. 2020. Synthetic 4-Hydroxy Auxarconjugatin B, a Novel Autophagy Inducer, Attenuates Gouty Inflammation by Inhibiting the NLRP3 Inflammasome. 2. *Cells* **9**:279.
27. **Andreu N, Phelan J, de Sessions PF, Cliff JM, Clark TG, Hibberd ML**. 2017. Primary macrophages and J774 cells respond differently to infection with Mycobacterium tuberculosis. *Sci Rep* **7**:42225.
28. **Zhao Z, Xu Y**. 2010. An extremely simple method for extraction of lysophospholipids and phospholipids from blood samples. *J Lipid Res* **51**:652–659.
29. **Fic E, Kedracka-Krok S, Jankowska U, Pirog A, Dziedzicka-Wasylewska M**. 2010. Comparison of protein precipitation methods for various rat brain structures prior to proteomic analysis. *ELECTROPHORESIS* **31**:3573–3579.
30. **Jiang L, He L, Fountoulakis M**. 2004. Comparison of protein precipitation methods for sample preparation prior to proteomic analysis. *Journal of Chromatography A* **1023**:317–320.
31. **Saravanan RS, Rose JKC**. 2004. A critical evaluation of sample extraction techniques for enhanced proteomic analysis of recalcitrant plant tissues. *PROTEOMICS* **4**:2522–2532.
32. **Thi Tran U, Kitami T**. 2019. Niclosamide activates the NLRP3 inflammasome by intracellular acidification and mitochondrial inhibition. *Commun Biol* **2**:2.
33. **Lai M, Yao H, Shah SZA, Wu W, Wang D, Zhao Y, Wang L, Zhou X, Zhao D, Yang L**. 2018. The NLRP3-Caspase 1 Inflammasome Negatively Regulates Autophagy via TLR4-TRIF in Prion Peptide-Infected Microglia. *Front Aging Neurosci* **10**:116.
34. **Li L-H, Ju T-C, Hsieh C-Y, Dong W-C, Chen W-T, Hua K-F, Chen W-J**. 2017. A synthetic cationic antimicrobial peptide inhibits inflammatory response and the NLRP3 inflammasome by neutralizing LPS and ATP. *PLoS One* **12**:e0182057.
35. **De la Roche M, Hamilton C, Mortensen R, Jeyaprakash AA, Ghosh S, Anand PK**. 2018. Trafficking of cholesterol to the ER is required for NLRP3 inflammasome activation. *J Cell Biol* **217**:3560–3576.
36. **Alphonse MP, Duong TT, Shumitzu C, Hoang TL, McCrindle BW, Franco A, Schurmans S, Philpott DJ, Hibberd ML, Burns J, Kuijpers TW, Yeung RSM**. 2016. Inositol-Triphosphate 3-Kinase C Mediates Inflammasome Activation and Treatment Response in Kawasaki Disease. *The Journal of Immunology* **197**:3481–3489.
37. **Kumari S, Khan S, Gupta SC, Kashyap VK, Yallapu MM, Chauhan SC, Jaggi M**. 2018. MUC13 contributes to rewiring of glucose metabolism in pancreatic cancer. 2. *Oncogenesis* **7**:1–12.
38. **Sakamoto S, Miyara M, Sanoh S, Ohta S, Kotake Y**. 2017. Mild MPP+ exposure-induced glucose starvation enhances autophagosome synthesis and impairs its degradation. 1. *Sci Rep* **7**:46668.
39. **Gómez de Cedrón M, Acín Pérez R, Sánchez-Martínez R, Molina S, Herranz J, Feliu J, Reglero G, Enríquez JA, Ramírez de Molina A**. 2017. MicroRNA-661 modulates redox and metabolic homeostasis in colon cancer. *Mol Oncol* **11**:1768–1787.
40. **Finucane OM, Sugrue J, Rubio-Araiz A, Guillot-Sestier M-V, Lynch MA**. 2019. The NLRP3 inflammasome modulates glycolysis by increasing PFKFB3 in an IL-1β-dependent manner in macrophages. 1. *Sci Rep* **9**:4034.
41. **Sanman LE, Qian Y, Eisele NA, Ng TM, van der Linden WA, Monack DM, Weerapana E, Bogyo M**. 2016. Disruption of glycolytic flux is a signal for inflammasome signaling and pyroptotic cell death. *eLife* **5**:e13663.
42. **Zhang X, Wang R, Hu D, Sun X, Fujioka H, Lundberg K, Chan ER, Wang Q, Xu R, Flanagan ME, Pieper AA, Qi X**. 2020. Oligodendroglial glycolytic stress triggers inflammasome activation and neuropathology in Alzheimer's disease. *Science Advances* **6**:eabb8680.